Pure Appl. Geophys.

https://doi.org/10.1007/s00024-021-02850-8

Pure and Applied Geophysics

Global Seismic Noise Wavelet-based Measure of Nonstationarity

Alexey Lyubushin[1]

Abstract—The properties of low-frequency global seismic noise, represented by continuous records for 24 years, 1997–2020, are investigated at 229 broadband stations located around the world. The property of waveforms, known as the Donoho–Johnston threshold, which separates the absolute values of the orthogonal wavelet coefficients into "small" and "large" is analyzed. The ratio of the number of "large" coefficients to their total number is determined by the dimensionless DJ index, which takes values from 0 to 1. The DJ index is considered as a measure of the nonstationarity of noise: the larger is the DJ index, the more is nonstationary the waveform. For each station, daily DJ index values are calculated. An auxiliary network of 50 reference points is introduced, the positions of which are determined by clustering the positions of seismic stations. For each reference point, a time series is constructed with a time step of 1 day, which is calculated as the median of daily DJ index values from the 5 nearest operable stations. For all pairs of reference points, the coherence between the DJ index values is estimated in a sliding time window of 365 days with an offset of 3 days, and the maximum values of the coherence function and the frequency at which the maximum coherence is reached are determined. The average values of the maximum coherences show strong growth after 2003, and the maximum distances between the reference points, for which the maximum coherence exceeded the threshold of 0.9, undergo an explosive increase in values after 2012. By extrapolating and averaging the DJ index values at the reference points, the region of concentration of maximum DJ index values was determined at the North-East Siberia. The bursts in the mean value of the maximum coherences between the day length and the DJ index values at the control points precede the release of seismic energy with a delay of about 530 days.

Keywords: Seismic noise, wavelet-based entropy, wavelet-based Donoho–Johnstone Index, coherence, vector autoregression, length of day.

1. Introduction

Seismic noise is considered as a source of information about the processes occurring in the lithosphere. In the works (Ardhuin et al., 2011; Aster et al., 2008; Kedar et al., 2008; Kobayashi & Nishida, 1998; Nishida et al., 2008, 2009; Rhie & Romanowicz, 2004; Tanimoto, 2001, 2005) it was shown that the source of the energy of low-frequency seismic noise is the processes occurring in the ocean and atmosphere, including those associated with climate change. Since the earth's crust is a medium for the propagation of seismic waves, changes in the lithosphere are reflected in the statistical properties of noise. Analysis of changes in these properties makes it possible to assess the effects associated with the seismic process occurring in different regions of the Earth and at the global level.

The article continues the research carried out in Lyubushin (2014, 2015, 2018, 2020a, c) on the study of the correlation and coherent properties of low-frequency seismic noise on a global scale, covering the entire planet. Since 1997, the total number of broadband seismic stations from various networks has become quite large (229 stations), and their location provides satisfactory coverage of the earth's surface. This makes it possible to evaluate the spatial and temporal correlations of various properties of seismic noise and to compare the revealed features with the seismic process. Multifractal characteristics (the singularity spectrum support width and the generalized Hurst exponent), as well as the minimum entropy of the distribution of the squares of the orthogonal wavelet coefficients were considered as the properties of seismic noise. These noise statistics were estimated for each station at successive 1 day intervals. An auxiliary network of 50 reference points distributed over the Earth's surface is introduced. For each of them the daily time series of the median values of seismic noise properties from the 5 nearest operable stations were calculated. In a sliding time window of 365 days, the mean of the moduli of the

[1] Institute of Physics of the Earth, Russian Academy of Sciences, Moscow, Russia. E-mail: lyubushin@yandex.ru

Published online: 26 August 2021

pairwise correlation coefficients of the daily noise properties between the values at all reference points were estimated. It turned out that the behavior of the average correlations for all properties has a common qualitative feature: until 2003, there is a decline, but after 2003, a rapid increase in correlation begins, which continues to this day. In Lyubushin (2020a, c), it was hypothesized that the break in the trends of average correlation in 2003 was caused by a high-frequency anomaly in the Earth's rotation regime, which can also trigger an increase in the intensity of the strongest seismic events after the Sumatran mega-earthquake on December 26, 2004. A break in the correlation trend in 2003 is accompanied by a break in the trends of the analyzed properties of seismic noise: after 2003, the averaged singularity spectrum support width decreases, while the averaged values of the noise entropy increases. This behavior of the properties of seismic noise (simplification of the statistical structure) is an indicator of an increase in seismic hazard (Lyubushin, 2018, 2021a, b). Thus, the simplification of the statistical structure of seismic noise and an increase in their spatial correlations occur synchronously, and this behavior can be interpreted as an increase in the global seismic hazard.

This article discusses another property of seismic noise, which is known in wavelet analysis as the Donoho–Johnston threshold. This threshold formally divides the set of orthogonal wavelet coefficients into "small" and "large" in terms of the magnitude of their absolute values. The ratio of the number of "large" wavelet coefficients to their total number is called the Donoho–Johnston Index (DJ index) and is interpreted as a measure of the unsteady behavior of the waveform of seismic noise. DJ index is also a measure of the complexity of a noise signal: if this index is small, then the signal is considered stationary, and its structure is simple.

The basis for interpreting the DJ index as a measure of the nonstationarity of a random signal is its difference from stationary Gaussian white noise, which is considered as a standard for a stationary random signal. For Gaussian white noise, the DJ index is practically zero. For instance, the author generated an example of stationary Gaussian white noise with unit variance one million samples long and estimated the change in the DJ index in successive 365-samples windows (the same one used in the article). As a result, the average value of such DJ index estimates turned out to be 0.002, the median is 0 exactly, the standard deviation is 0.002, and the maximum value is 0.003.

The experience of using the DJ index has shown that it is more sensitive to changes in the properties of the seismic noise field than the previously used multifractal and entropic properties of noise. In particular, the DJ index is characterized by higher spatial correlations. In addition, instead of analyzing the pairwise coefficients between the properties of the noise at the reference points, this article considers estimates of pairwise frequency-dependent coherence functions. For each coherence function, the maximum values and frequencies realizing these maxima are found. The transition from conventional correlation coefficients to frequency-dependent coherence functions allows increasing the threshold of the measure of connectivity of property values at different reference points and revealing other non-obvious properties of seismic noise.

Another innovation of the described approach is the analysis of the coherence between the unevenness of the Earth's rotation, represented by the time series of the length of the day (LOD) and the DJ index values at each control point. Thus, the "response field" of the seismic noise properties on the LOD is considered. Previously, for this purpose, the coherences between LOD and mean values of noise properties or the first principal component of several properties were analyzed (Lyubushin et al., 2021; Lyubushin, 2020b, 2021b). Averaging the coherence functions between the LODs and the noise properties in the control point network provides a better estimate of the effect of advancing the coherence bursts relative to the bursts in the released seismic energy values. Earlier, this advance effect was found for global seismicity (Lyubushin, 2020c), for Kamchatka (Lyubushin et al., 2021), and for Japan (Lyubushin, 2021b).

2. *Seismic Data*

The data used are the vertical components of continuous seismic noise records with a sampling

time interval of 1 s, which were uploaded from the Incorporated Research Institutions for Seismology (IRIS) website at http://www.iris.edu/forms/webrequest/ with 229 broadband seismic stations of 3 networks: http://www.iris.edu/mda/_GSN, http://www.iris.edu/mda/G, http://www.iris.edu/mda/GE.

Seismic noise records with a sampling rate of 1 Hz (LHZ records) were reviewed for 24 years of recording (January 1, 1997 to December 31, 2020). These data were converted to a time series with a time step of 1 min by calculating averages for successive time intervals of 60 s.

Let's consider an auxiliary network of 50 reference points, which are determined using the hierarchical cluster analysis of the positions of 229 seismic stations using the far-neighbor method. This method of cluster analysis allows the formation of compact clusters (Duda et al., 2000). The location of 229 seismic stations and 50 control points is shown in Fig. 1.

3. Wavelet-based Donoho–Johnstone Index

Let $x(t)$ be a time series of a random signal and let $t = 1, \ldots, N$ be an integer index numbering consecutive data points (discrete time). The normalized final sample entropy is determined by the following formula:

$$En = -\sum_{k=1}^{N} p_k \cdot \log(p_k)/\log(N), \quad p_k = c_k^2/\sum_{j=1}^{N} c_j^2, \quad 0 \le En \le 1 \tag{1}$$

where c_k are orthogonal wavelet coefficients. Let us choose the optimal orthogonal wavelet for the sample

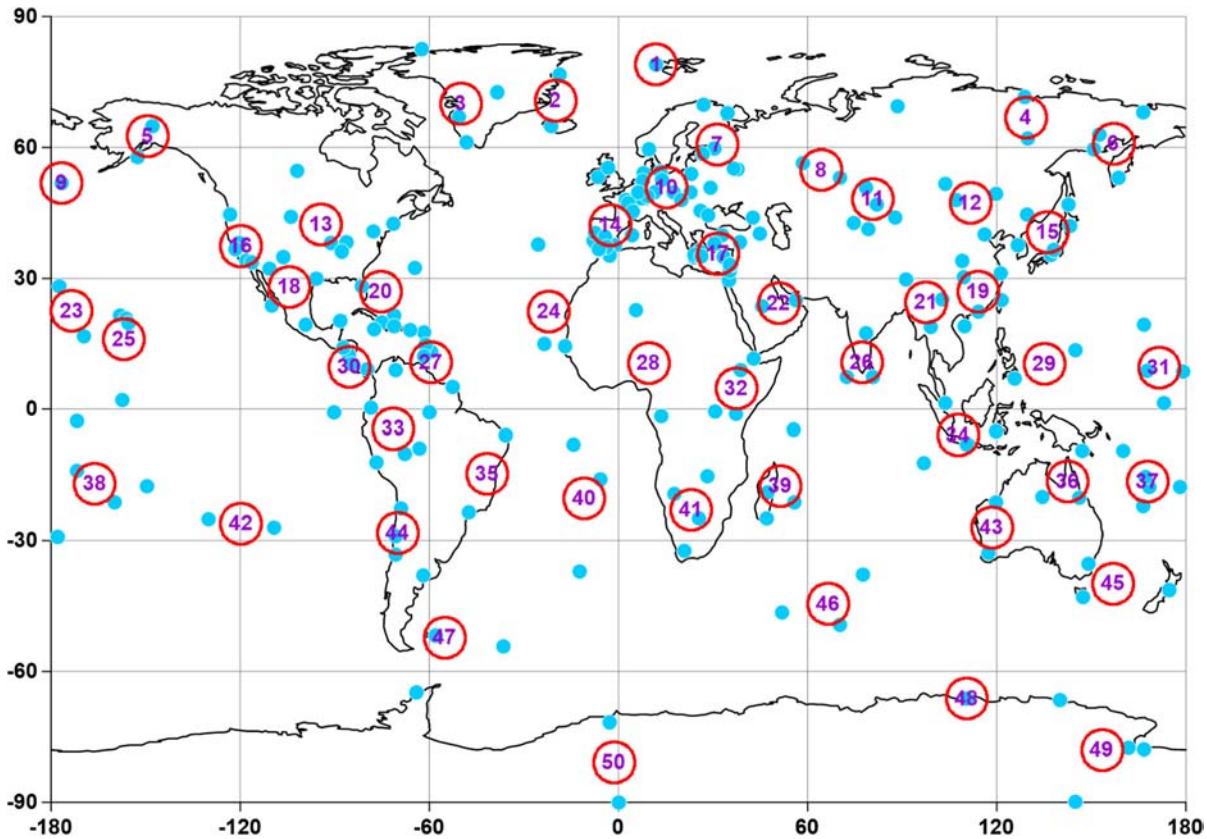

Figure 1
Positions of 229 broadband seismic stations are presented by blue circles; red numbered circles present 50 reference points

under consideration from the entropy minimum condition (1) on a finite set of Daubechies wavelet bases (Mallat, 1999) with the number of vanishing moments from 1 to 10.

The entropy of seismic noise (1) has been repeatedly used in Lyubushin (2014, 2015, 2017, 2018, 2020a, 2020b, 2020c, 2021a; b) to analyze seismic noise for different regions of the Earth and at the global level as an independent tool. By its construction, entropy (1) is also multiscale, like the entropy proposed in Costa et al., (2003, 2005) for studying the properties of random signals. In the works Koutalonis and Vallianatos (2017), Vallianatos et al. (2019), the non-extensive Tsallis entropy was used to analyze seismic noise. The natural time approach to the analysis of random data uses a related definition of entropy in Varotsos et al., (2003a, 2003b). But in this work, entropy (1) acts not as the main tool for data analysis, but as some auxiliary stage of data processing, which is designed to determine the optimal wavelet basis.

After the wavelet basis for a given signal is determined from the entropy minimum condition, we can determine the set of wavelet coefficients that are the smallest in absolute value. In wavelet filtering, these wavelet coefficients can be zeroed before the inverse wavelet transform in order to "reduce noise" (Donoho & Johnstone, 1995; Mallat, 1999). We assume that the noise is concentrated mainly in the variations at the first level of detail. Recall that the first level of detail corresponds to the highest frequency variations of the time series with periods from 2Δt to 4Δt, where Δt is the time sampling step. Due to the orthogonality of the wavelet transform, the variance of the wavelet coefficients is equal to the variance of the original signal. Thus, we estimate the standard deviation of the noise as the standard deviation of the wavelet coefficients at the first level of detail. This assessment must be robust, i.e. insensitive to outliers in the values of the wavelet coefficients at the first level. To do this, we can use a robust median estimate of the standard deviation for a normal random variable:

$$\sigma = \mathrm{med}\left\{\left|c_k^{(1)}\right|, \quad k = 1, ..., N/2\right\} \Big/ 0.6745 \qquad (2)$$

here $c_k^{(1)}$ are wavelet coefficients at the first detail level of orthogonal wavelet decomposition which corresponds to most high-frequency variations of the signal, formally with periods from $2\Delta t$ up to $4\Delta t$ where Δt is sampling time step (in our case it equals 1 min); $N/2$ is the number of such coefficients. The 1st detail level is considered as the noisiest—that is why the noise component standard deviations is estimated from its wavelet coefficients. The estimate of the standard deviation σ from formula (2) defines the value $\sigma\sqrt{2 \cdot \ln N}$ as the "natural" threshold for the extraction of noise wavelet coefficients. The quantity $\sigma\sqrt{2 \cdot \ln N}$ is known in wavelet analysis as the Donoho–Johnston threshold, and the expression itself for this quantity is based on the formula for the asymptotic probability of maximum deviations of Gaussian white noise. As a result, it is possible to determine the dimensionless characteristic (*DJ index*) of the signal γ, $0 < \gamma < 1$, as the ratio of the number of the most informative wavelet coefficients for which the inequality $|c_k| > \sigma\sqrt{2 \cdot \ln N}$ is satisfied to the total number N of all wavelet coefficients. Formally, the larger is the index γ, the more informative (less "noisy") is the signal. Further, the DJ index values are interpreted as a measure of seismic noise non-stationarity.

Figure 2 shows graphs of daily DJ index values for each control point, calculated as median values from the five nearest stations that are operational on each day. Before calculating the minimum entropy (1) and index (2), the trend is removed from the daily waveforms of seismic noise by an 8th order polynomial. Removing the trend is necessary to get rid of the influence of tides and daily temperature effects.

The presence of values at 50 points distributed around the world allows to build a map of the spatial distribution of the DJ index. To build a map, consider a regular grid of 50 nodes in latitude and 100 nodes in longitude, covering the entire earth's surface. Let ζ_k, $k = 1, \ldots, m$ be the coordinates of the control points (in our case $m = 50$), Z_k are the DJ index values at the reference points #k, r are the coordinates of the nodes of the regular grid, $d(\zeta_k, r)$ is the distance on the surface of the spherical Earth between

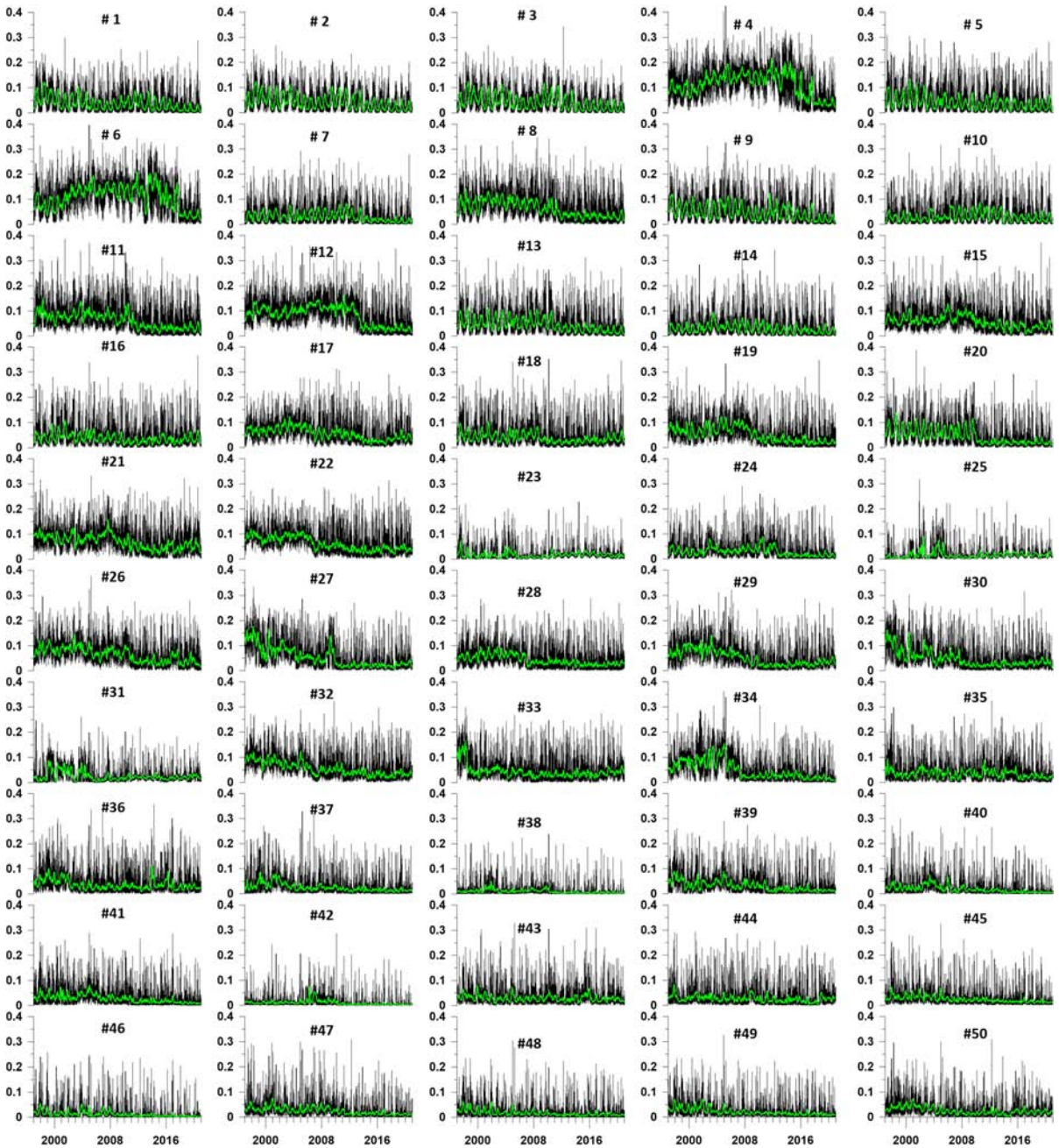

Figure 2
Graphs of daily values of wavelet-based DJ index for 50 reference points. Green lines present sliding average within window 57 days

the points ζ_k and r, h is the smoothing radius (bandwidth) of the Gaussian kernel function. Then the values at the nodes of the regular grid are calculated by the formula [Duda et al., 2000]:

$$\hat{Z}(r) = \sum_{k=1}^{m} Z_k \exp\left(-d^2(\zeta_k, r)/h^2\right) \Big/ \sum_{k=1}^{m} \exp\left(-d^2(\zeta_k, r)/h^2\right). \tag{3}$$

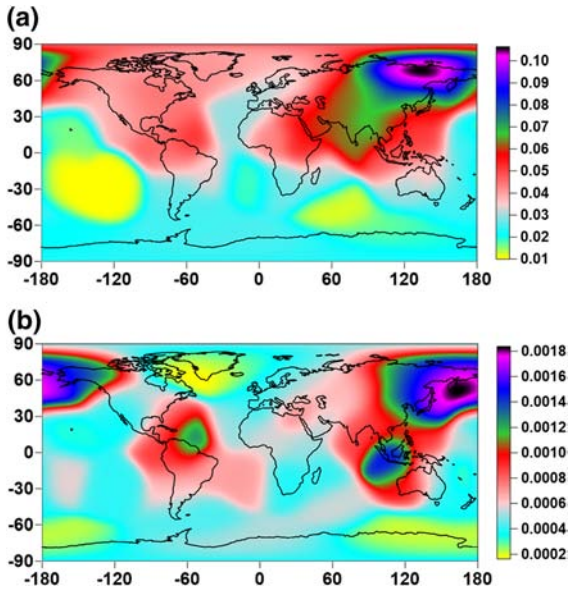

Figure 3
a Average map of spatial distribution of seismic noise DJ index obtained by extrapolation from 50 reference points using Gaussian kernel with bandwidth 15°; **b** map of variance of kernel estimate

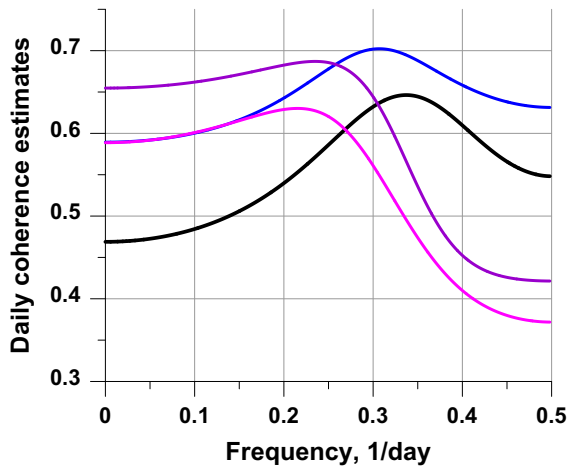

Figure 4
Examples of four estimates of the coherence functions between daily values of DJ indices at two reference points in a 365-day window

The value of the bandwidth $h = 15^\circ$ was used, which corresponds to a distance of $\approx$ 1700 km. The values $\hat{Z}(r)$ calculated on a daily basis at all nodes provide a daily map of the DJ index spatial distribution. The result of averaging all daily maps is shown in Fig. 3a. Figure 3b presents map of variance of kernel estimate which is obtained by averaging Gaussian kernel estimates of the squared deflections of daily kernel estimates from values of DJ-index within reference points.

Figure 3a shows an area of concentration of large DJ index of seismic noise waveforms in the North-East of Siberia for geographic coordinates approximately in a rectangle, $62^\circ \le \mathrm{Lat} \le 74^\circ$, $116^\circ \le \mathrm{Lon} \le 151^\circ$.

4. *Coherence Measure for Reference Points Network*

Earlier in Lyubushin (2020a, 2020c), a network of 50 reference points, shown in Fig. 1, was used to calculate the absolute values of pairwise correlation coefficients between daily values of various properties of seismic noise. In this article, instead of the correlation coefficients, the coherence functions are calculated. The transition from simple correlations to frequency-dependent coherence functions makes it possible to single out the frequency values for which the coherence reaches its maximum values. Thus, additional information appears about the structure of spatial relationships between the values of the properties of seismic noise. Besides that, searching for coherence maxima over frequency values increases the degree of coupling between noise properties values at different reference points as compared to a simple correlation coefficient.

To calculate the coherence function, we use the vector autoregression model (Marple, 1987):

$$Z(t) + \sum_{k=1}^{p} A_k \cdot Z(t-k) = e(t) \qquad (4)$$

here $Z(t)$ is some q-dimensional time series, p is the order of autoregression, A_k is the $q \times q$ size autoregressive coefficient matrix, $e(t)$ is the residual signal with zero mean and $q \times q$ size covariance matrix $\Phi = M\{e(t)e^T(t)\}$. The model (4) is used for estimating coherence functions between values of DJ-index within all pairs of reference points—that is why $q = 2$ for our case. The matrices A_k and Φ are determined using the Durbin-Levinson procedure (Marple, 1987), and the spectral matrix is calculated by the formula:

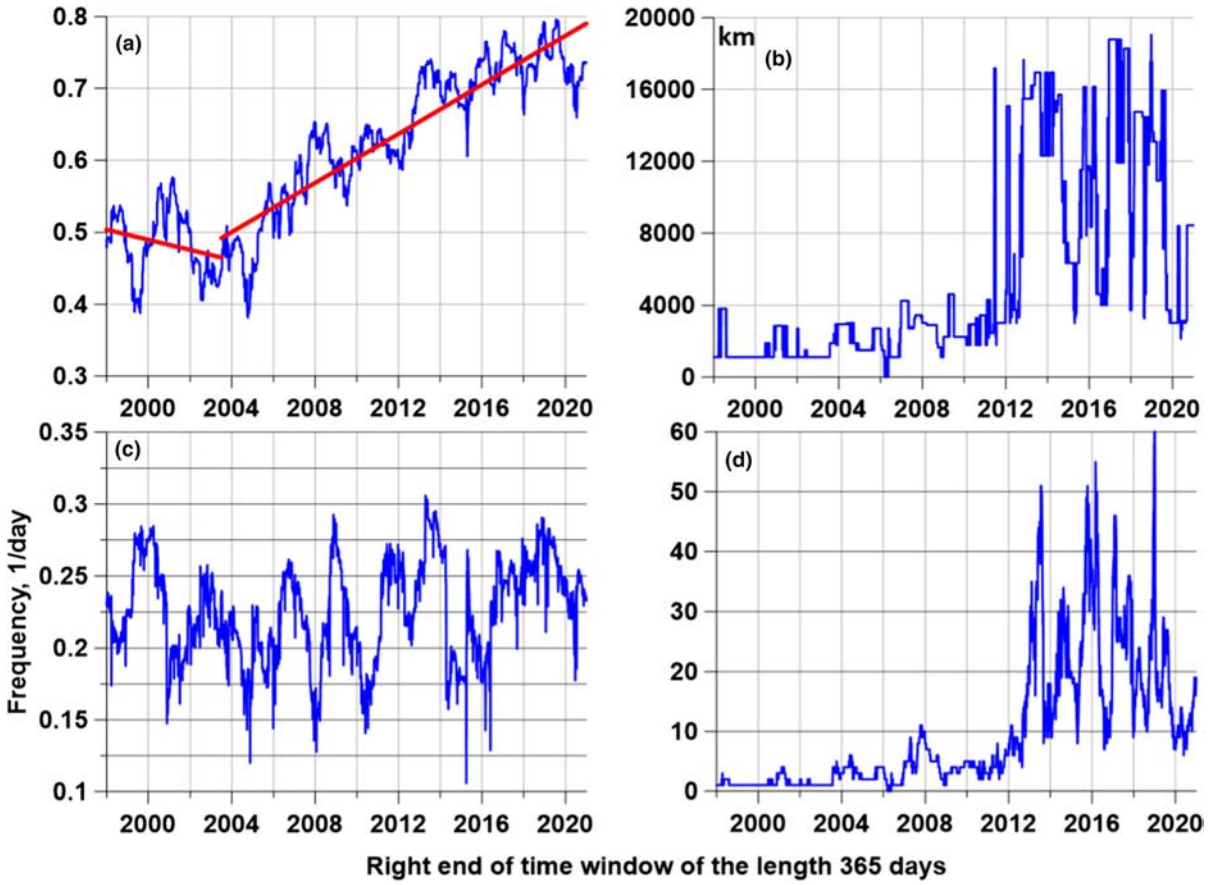

Figure 5
a The average values $\overline{\mu}(\tau)$ of the maxima over the frequency of the modules of all pairwise coherences; red lines present linear trends before and after 2003.5; **b** maxima $\rho(\tau)$ of distances between reference points for which coherence maximum exceeds the threshold 0.9; **c** mean frequencies $\overline{\omega}(\tau)$ for which pairwise coherences attain maxima; **d** number $n(\tau)$ of pairs of reference points for which coherence maximum exceeds the threshold 0.9

$$S_{ZZ}(\omega) = \Psi^{-1}(\omega) \cdot \Phi \cdot \Psi^{-H}(\omega),$$
$$\Psi(\omega) = I + \sum_{k=1}^{p} A_k e^{-i\omega k} \tag{5}$$

where I is the unit size $q \times q$ matrix. When $q = 2$, then the value (5) equals to the usual spectrum of coherence:

$$\lambda(\omega) = |S_{12}(\omega)| \Big/ \sqrt{S_{11}(\omega) \cdot S_{22}(\omega)} \tag{6}$$

where $S_{11}(\omega)$ and $S_{22}(\omega)$ are the diagonal elements of matrix (5), that is, parametric estimates of the power spectra of two signals, and $S_{12}(\omega)$ is their mutual cross-spectrum.

To calculate pairwise coherence functions (6) between the DJ index values at the reference points, a second-order autoregressive model was used with a preliminary transition to increments. The choice of a low order of autoregression $p = 2$ was aimed at suppressing random fluctuations in coherence estimates and obtaining smooth dependences on frequency. The calculations were performed in sliding time windows 365 days in length with an offset of 3 days. Figure 4 shows examples of graphs of estimates of pairwise coherence functions.

Let us denote by $\lambda_{ij}^{(\tau)}(\omega)$ the estimate of the coherence function between the DJ index values at the reference points with the numbers i and j for the window with the time stamp τ of the right end. Let

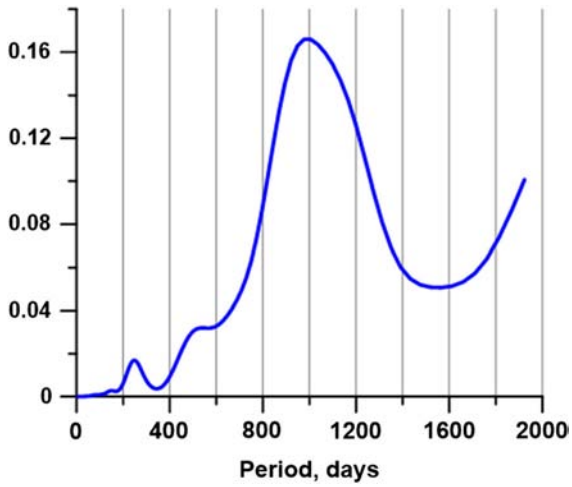

Figure 6
Graph of logarithm of squared Morlet wavelet coefficients for average values $\overline{\mu}(\tau)$ of the maxima over frequency of all pairwise absolute coherences

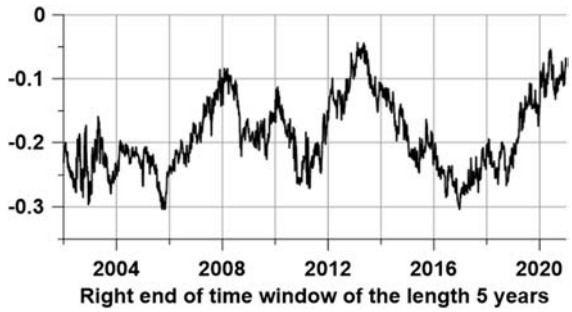

Figure 7
Robust correlation coefficient between increments of averaged values of mean maximum coherences $\overline{\mu}(\tau)$ and mean frequencies $\overline{\omega}(\tau)$ providing coherence maxima within time window of the length 1826 days (5 years). Correlation coefficients are negative what mean that increasing of mean coherence maxima accompanies decreasing of mean frequency

$\mu_{ij}^{(\tau)} = \max_{\omega} \lambda_{ij}^{(\tau)}(\omega)$, $\omega_{ij}^{(\tau)}$ be the value of the frequency at which the maximum is reached. Let's calculate the average values for all pairs of reference points:

$$\overline{\mu}(\tau) = \sum\nolimits_{(i,j)} \mu_{ij}^{(\tau)}/M, \quad \overline{\omega}(\tau) = \sum\nolimits_{(i,j)} \omega_{ij}^{(\tau)}/M \quad (7)$$

In the formula (7) $M = m(m-1)/2$ is the number of different pairs of control points from their total number. In our case $m = 50$, $M = 1225$. Let us select those pairs of control points for which the maximum coherence $\mu_{ij}^{(\tau)}$ in the current time window τ has exceeded the threshold 0.9 and denote by $n(\tau)$ the total number of such pairs in each time window. In addition, let us denote by $\rho(\tau)$ the maximum distances between those pairs of reference points for which the maximum coherence exceeds the threshold 0.9. Dependencies $\overline{\mu}(\tau)$, $\overline{\omega}(\tau)$, $n(\tau)$ and $\rho(\tau)$ are shown in Fig. 5.

In the dependence $\overline{\mu}(\tau)$ in Fig. 5a, attention is drawn to the break in the trend in the vicinity of the time point of the right end of the annual window 2003.5. This feature is highlighted by the line trend graphs plotted before and after mid-2003 (red lines). After 2003.5, the average maximum coherence began to grow rapidly. This inflection point in the trend has previously been found for the behavior of the mean of the absolute values of pairwise correlations, estimated in a sliding time window of 365 days, for other daily seismic noise properties (Lyubushin, 2020a, 2020c). As the reason for the change in the trend in the correlation of the properties of seismic noise, these works proposed a hypothesis about the trigger effect of a high-frequency anomaly in the Earth's rotation mode, which can also cause an increase in the intensity of the world's strongest earthquakes after the Sumatran mega-earthquake of December 26, 2004.

Also noteworthy is the periodic structure of fluctuations in magnitude of $\overline{\mu}(\tau)$ around linear trends in Fig. 5a. To determine the period of these oscillations, let us calculate the logarithm of the mean value of the squared moduli of the Morlet wavelet coefficients (Mallat, 1999) of the dependence $\overline{\mu}(\tau)$, the graph of which is shown in Fig. 6. On this graph, a period of about 1000 days (2.7 years) is highlighted. Further, this result will be discussed in connection with the periodic structure of the global seismic process.

Returning to Fig. 5, let us pay attention to the graphs of the dependences $\rho(\tau)$ of the maximum distances between the control points with strong coherence and the number $n(\tau)$ of pairs of such points (Fig. 5b and e). For both dependences, after the time right point of the annual window 2012, the regime of high-frequency chaotic fluctuations with high amplitude begins. Earlier, a similar regime with the beginning around 2010 was already identified for the maximum distances between the reference points with the absolute correlation of the noise entropy (1)

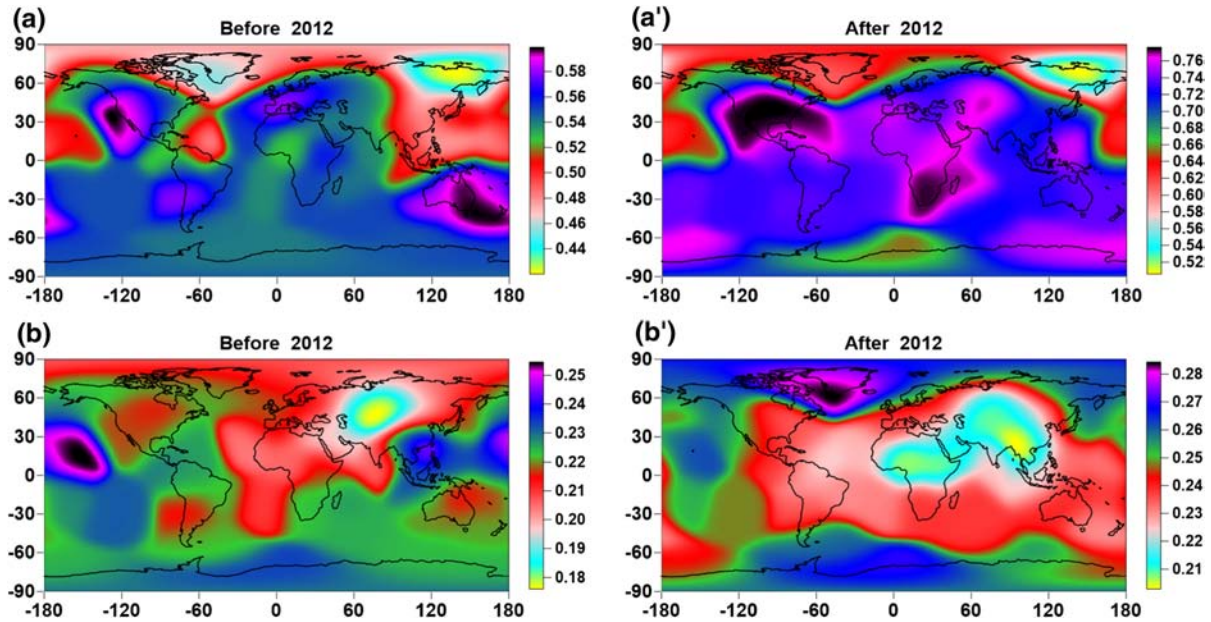

Figure 8
Averaged maps of spatial distribution of mean maximum coherences $\overline{\mu}_j(\tau)$ (**a** and **a**') and mean frequencies $\overline{\omega}(\tau)$, providing maximum coherence (**b** and **b**') for estimates with right end of time windows before (**a** and **b**) and after (**a**' and **b**') 2012. Maps were obtained by extrapolation from 50 reference points using Gaussian kernel with bandwidth 15°

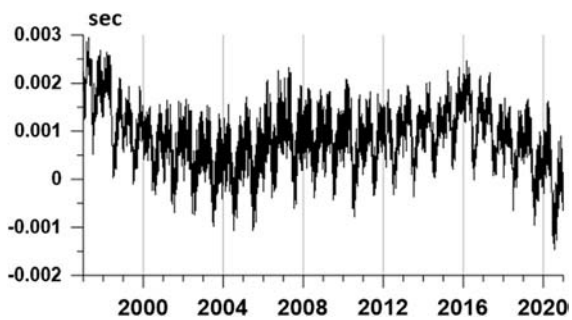

Figure 9
Graph of length of day

exceeding the threshold of 0.7 (Lyubushin, 2020c). However, the behavior of the quantity for the maximum coherence between the values of DJ index (2) is much more expressive and is emphatically "explosive" (in sense of the magnitude of the differences between the amplitude of fluctuations before and after the onset of the regime of chaotic fluctuations) than for entropy (1). In Lyubushin (2020c), the appearance of sharp bursts in the values of the maximum distance between pairs of reference points with a strong correlation of entropy is associated with the destabilization of the seismic noise field after two mega-earthquakes close in time: February 27, 2010, M = 8.8 in Chile and 11 March 2011, M = 9.1 in Japan.

Comparing the synchronous graphs of quantities and in Fig. 5a and c, it can be seen that they are "antiphase": an increase in the maximum coherence $\overline{\mu}(\tau)$ in Fig. 5a is accompanied by a decrease in the average frequency $\overline{\omega}(\tau)$ in Fig. 5c, in which the maximum of coherence is realized. In order to quantitatively check this observation, let us calculate the evolution of the correlation coefficient between the increments of values $\overline{\mu}(\tau)$ and $\overline{\omega}(\tau)$ in a certain sliding time window. Since both values themselves represent estimates in a sliding time window of 365 days with an offset of 3 days, then if we take a window consisting of adjacent L values of correlated quantities, then the dimensional length of this "large" window will be equal to $365 + 3(L - 1)$ days. If we choose the length of the "large" window equal to $L = 488$ the adjacent values of statistics $\overline{\mu}(\tau)$ and $\overline{\omega}(\tau)$, then the dimensional length of this window will

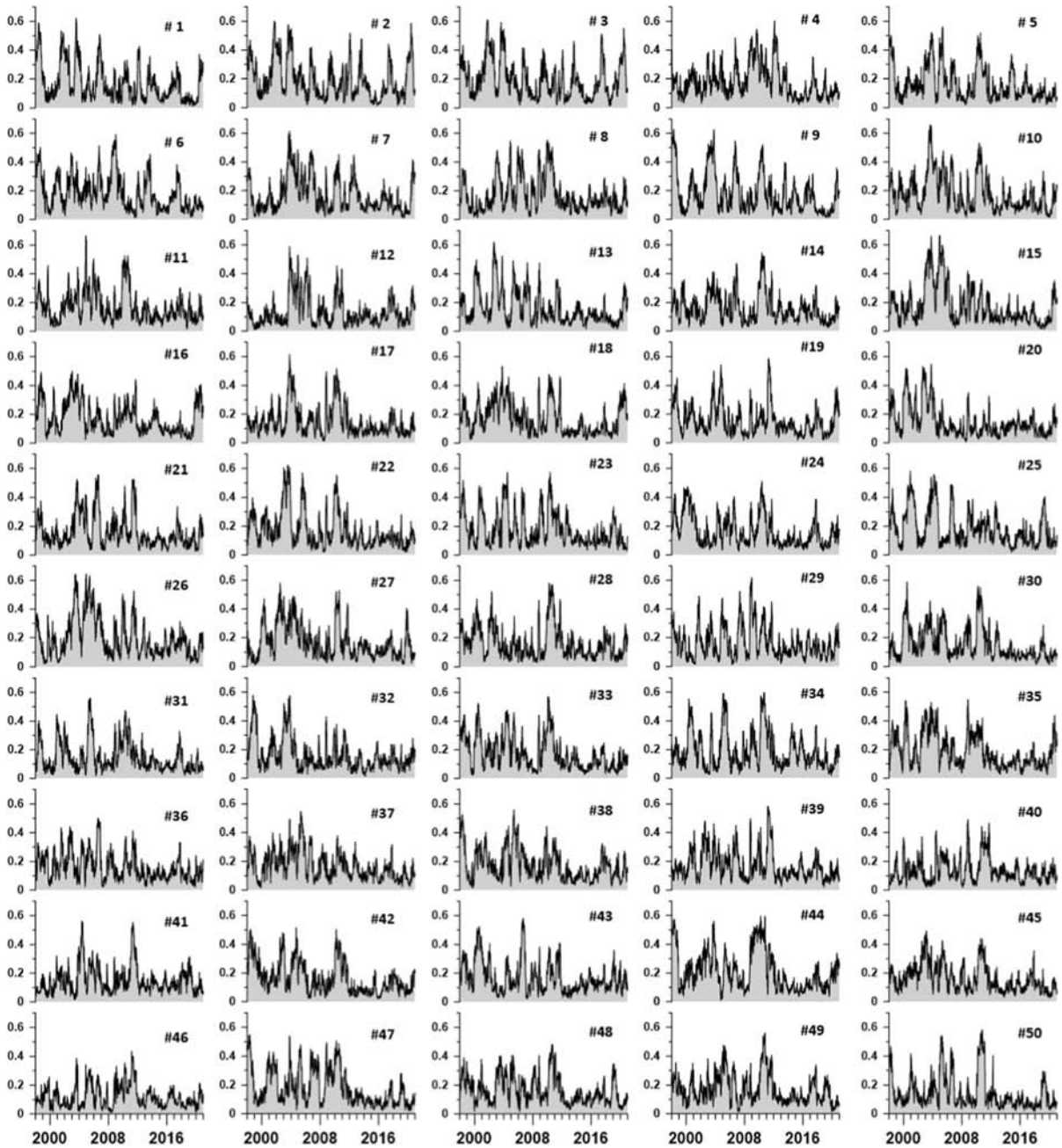

Figure 10
Graphs of maxima squared coherences between daily median values of seismic noise wavelet-based DJ indices in 50 reference points over the world and LOD time series estimated within moving time window of the length 365 days with mutual shift 3 days. Graphs were plotted in dependence on the right-hand end of moving time window

be equal to 1826 days, which corresponds to 5 years (taking into account that every 4th year is a leap year).

When calculating the correlation coefficient between the increments of $\overline{\mu}(\tau)$ and $\overline{\omega}(\tau)$, it should be taken into account that the increments of the average

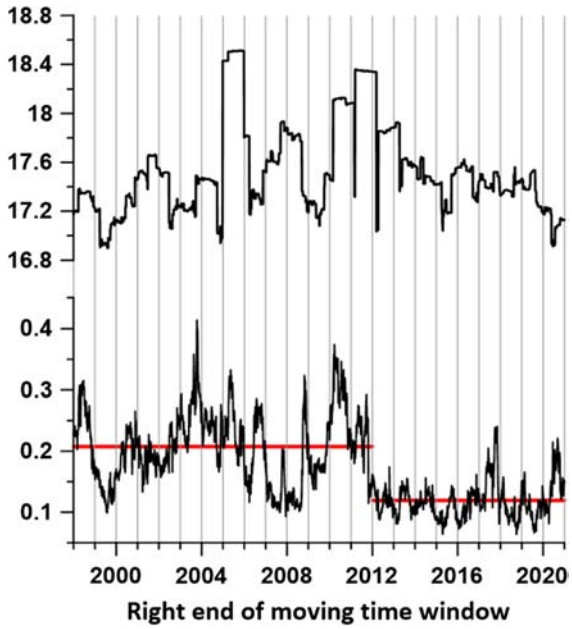

Figure 11
a Plot of the decimal logarithm of released seismic energy; **b** mean value of maximum coherences between daily median DJ indices in 50 reference points and length of day. Graphs **a** and **b** are plotted within time window of the length 365 days with mutual shift 3 days. Red horizontal lines on the **b** present mean values of coherence maxima for right hand ends of time windows before and after 2012

frequency $\overline{\omega}(\tau)$ contain significant outliers. Therefore, instead of the usual Pearson correlation coefficient, we used the formula for the robust correlation coefficient between random variables u and w (Huber & Ronchetti, 2009):

$$r = \frac{S(\varphi^2) - S(\psi^2)}{S(\varphi^2) + S(\psi^2)}, \quad \varphi = \frac{u}{S(u)} + \frac{w}{S(w)}, \quad \psi = \frac{u}{S(u)} - \frac{w}{S(w)} \tag{8}$$

where $S(u) = med|u - med(u)|$, $med(u)$ is the median of the value u, $S(u)$ is the absolute median deviation of the value u.

Figure 7 shows a graph of the robust correlation coefficient (8) between the increments of $\overline{\mu}(\tau)$ and $\overline{\omega}(\tau)$, estimated in a sliding time window of 5 years. It can be seen that the estimate is negative for all time windows, which confirms the hypothesis that an increase in the maximum coherence leads to a decrease in the frequency at which this maximum coherence is realized.

At each reference point with the number j and for each time window τ, there are estimates of the average values $\overline{\mu}_j(\tau)$ of the maximum coherence between the DJ index values at this reference point and the values at the other reference points and estimates of the average values $\overline{\omega}_j(\tau)$ of the frequencies for which the maximum coherence is realized. The previously entered values $\overline{\mu}(\tau)$ and $\overline{\omega}_j(\tau)$ are the average of such pointwise values: $\overline{\mu}(\tau) = \sum_{j=1}^{m} \overline{\mu}_j(\tau)/m$, $\overline{\omega}(\tau) = \sum_{j=1}^{m} \overline{\omega}_j(\tau)/m$. The presence of estimates $\overline{\mu}_j(\tau)$ and $\overline{\omega}_j(\tau)$ at the reference points allows us to build maps of the distribution over the space of their values using a Gaussian averaging kernel similar to formula (3) with the same value of the bandwidth $h = 15°$. These maps are shown in Fig. 8. separately for labels of the right ends of time windows before and after 2012.

Note that in Fig. 8a and a', the Arctic region corresponds to the minimum values of the maximum coherences, and the area of the smallest values $\overline{\mu}_j(\tau)$ coincides with the area of maximum DJ index values in Fig. 3 and is located in the North-East of Eurasia. Thus, both statistics, the initial γ and the results of its subsequent processing $\overline{\mu}_j(\tau)$, highlight the same stable anomalous regions of the behavior of global seismic noise.

As for the frequency distribution maps, realizing the maximum coherence, presented in Fig. 8b and b', it follows from them that Antarctica is characterized by high frequencies, while for the center of Eurasia and equatorial Africa after 2012, low frequencies of maximum coherence are typical.

5. *Connection to Length of Day*

The uneven rotation of the Earth has long been the subject of geophysical research (Levin et al., 2017). Most often, the main reason for the irregular rotation is determined by the influence of processes in the atmosphere and ocean, as well as climatic changes (Zotov et al., 2017). The relationship between changes in the parameters of the Earth's rotation with the seismic process has been studied in many works, for example (Bendick & Blham, 2017; Shanker et al., 2001; Changy & Wenke, 2012). This work continues the study of the relationships between the properties

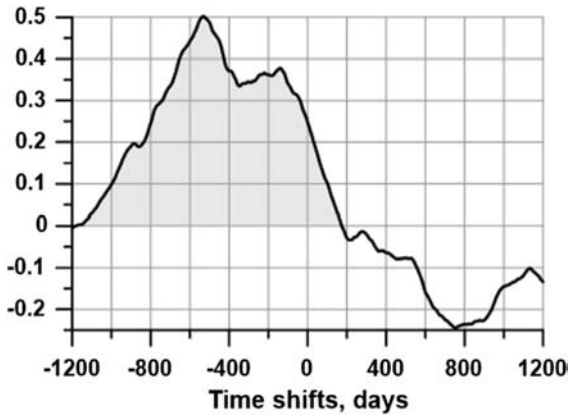

Figure 12
Correlation function between the values of the logarithm of the released seismic energy and the mean of maxima of coherence between the day length and DJ indices in 50 reference points. Negative values of time shifts on graph correspond to the lag in the release of seismic energy relative to bursts of coherence

of seismic noise with the irregularity of the Earth's rotation and with the process of discharge of accumulated seismic energy, carried out in Lyubushin (2020a, 2020b, 2020c), Lyubushin (2021a, 2021b), Lyubushin et al., (2021) at analysis of seismic noise at the global level, in Japan, California and Kamchatka.

Figure 9 shows a graph of the length of day (LOD) for the time interval 1997–2020. Data taken from the International Earth rotation and Reference systems Service (IERS) website at: https://hpiers.obspm.fr/iers/eop/eopc04/eopc04.62-now.

Previously, in Lyubushin (2020a, 2020b, 2020c), Lyubushin (2021a, 2021b), Lyubushin et al., (2021), to analyze the relationship between the properties of seismic noise, the maximum values of the quadratic spectrum of coherence between the increments of the LOD time series and the medians of the daily seismic noise calculated from all stations in the network in a sliding time window of 365 or 182 days were used. If several noise properties were analyzed, then their first principal component was calculated in a moving time window of the same length that was used to calculate the coherence spectrum. When evaluating in moving time windows, the values of the coherence spectra are concentrated mainly in a narrow frequency band with periods from 11 to 14 days. The maximum values of the coherences taken over all frequencies form a time sequence with a time step equal to the time window offset. It was shown in Lyubushin (2020c), Lyubushin (2021b), Lyubushin et al., (2021) that peaks of maximum values of coherence between LOD and seismic noise properties, on average, outstrip seismic energy emissions from earthquakes, which are calculated also in a sliding time window of the same length and taken with the same offset as when evaluating a sequence of coherence spectra. The time delay of seismic energy bursts relative to peaks of maximum coherence was estimated by calculating the cross-correlation function. Minimum entropy (1), as well as multi-fractal properties: the generalized Hurst exponent and the singularity spectrum support width were used as the properties of seismic noise. The Donoho-Johnston index was used to analyze the relationship with LOD on the Japanese Islands, but not separately, but in combination with the minimum entropy and the singularity spectrum support width. As a result of numerical experiments with various properties of global seismic noise, it turned out that DJ index demonstrates the most striking manifestations of the spatial and temporal correlation of seismic noise, as well as in its connection with the irregular rotation of the Earth.

In addition, in this paper, the coherence between LOD and seismic noise properties is calculated separately for each reference point and not for median values across all stations in the network. Thus, LOD is viewed as a kind of "probe signal", the response to which is distributed throughout the globe at reference points, which allows one to analyze the spatial characteristics of the "response" of seismic noise to LOD.

Figure 10 shows the graphs of the maximum quadratic coherence between the DJ index increments at the control points (Fig. 2) and the LOD time series increments (Fig. 9), calculated in sliding time windows 365 days in length with an offset of 3 days. To calculate pairwise coherence, the autoregressive model (4)–(6) for order $p = 5$ was used, similar to the estimates used in Lyubushin (2020a, 2020b, 2020c), Lyubushin (2021b), Lyubushin et al., (2021).

Figure 11 shows the graphs of two synchronous curves: Fig. 11a—the logarithm of the released seismic energy (in joules) in a sequence of time intervals 365 days in length, taken with an offset of 3 days;

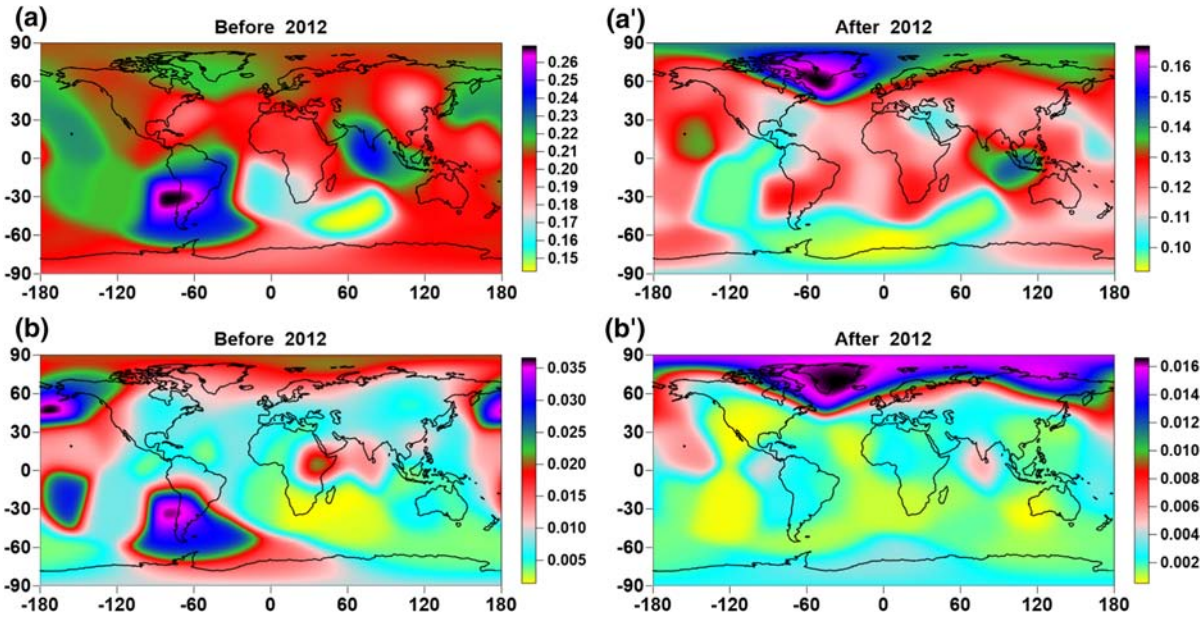

Figure 13
Averaged maps of spatial distribution of maximum coherences between LOD and DJ index (**a** and **a**') and their variances (**b** and **b**') for estimates with right end of time windows before (**a** and **b**) and after (**a**' and **b**') 2012. Maps were obtained by extrapolation from 50 reference points using Gaussian kernel with bandwidth 15°

Fig. 11b—mean values of maximum coherences between time series of day length and daily DJ index values at 50 reference points. The behavior of the curve in Fig. 11b can be divided into two sections with timestamps of the right ends of the windows before and after 2012, which differ significantly from each other by the mean values represented by the horizontal red lines. Note that the behavior of the maximum pairwise coherences exceeding the threshold of 0.9 and the maximum distances between such reference points in Fig. .5b and d are also very different for the time stamps of the right ends of the windows before and after 2012. Thus, the response of the properties of seismic noise DJ index to irregular rotation of the Earth (LOD time series) turned out to be dependent on the degree of spatial connectivity of the strong coherences of noise DJ index.

When comparing the curves in Fig. 11a and b, it can be seen that strong bursts of coherence precede significant bursts of seismic energy. To estimate the time shift between the two curves in Fig. 11, we calculate the correlation function between them. The graph of this correlation function is shown in Fig. 12 for time shifts of $\pm$ 1200 days. The correlation function has a significant asymmetry and is shifted to the region of negative time shifts, which correspond to the advance of the coherence maxima of the seismic energy emission maxima. The maximum correlation falls on a time shift of $-$ 530 days. Earlier, a similar effect of advancing coherence bursts between LOD and seismic noise properties was found in Lyubushin (2020c, 2021b), Lyubushin et al., (2021) for Japan, Kamchatka and for the whole world (for entropy as an analyzed property).

Figure 13a and a' show averaged spatial distribution maps of the coherence maxima between LOD and DJ index values for time intervals before and after 2012. The maps are obtained by extrapolating from a network of 50 reference points to the entire earth's surface using a Gaussian kernel function with bandwidth of 15 degrees. Averaging is performed according to formula (3) over all time windows 365 days in length with an offset of 3 days, the time stamps of the right ends of which have values before and after 2012. From a comparison of the maps in Fig. 13a and a', it can be seen that the scale of

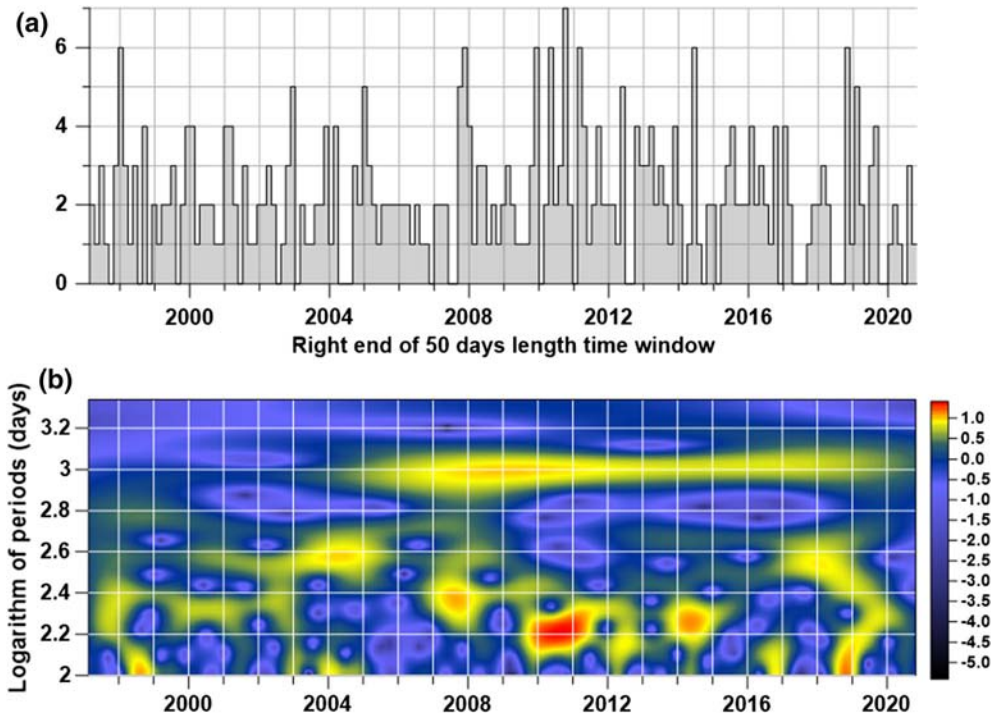

Figure 14
a Number of earthquakes with magnitude not less than seven within adjacent time fragments of the length 50 days; **b** time–frequency diagram of logarithm of squared Morlet wavelet coefficients of time series presented at **a**

changes in the DJ index response to the irregular rotation of the Earth after 2012 has decreased by almost 2 times (which corresponds to the graph in Fig. 11b). In addition, the areas of maximum response concentration moved from two spots on the Pacific coast of South America and in India before 2012 to the Arctic after 2012.

To assess the degree of stationarity of responses to LOD, Fig. 13b and b' show the distribution maps of the variances of the maximum coherences between LOD and DJ index, also separately before and after 2012. The variances were first calculated at reference points, and then extrapolated to the entire surface of the Earth using the Gaussian nuclear function, similar to the maps in Fig. 13a and a'. A significant change after 2012 is the migration of areas of concentration of high variance values also to the Arctic region.

6. Discussion

According to the conducted studies of the measure of non-stationary behavior of seismic noise, based on the use of the wavelet DJ index, two critical time intervals can be distinguished when the properties of seismic noise have changed significantly. Taking into account the fact that the properties of seismic noise are estimated in sliding time windows of 365 days, the critical time intervals are also determined with an accuracy of 1 year.

The first time interval 2002.5–2003.5 refers to the change in the trend of the average maximum coherence between the values of the noise properties at the reference points. After this interval, a systematic increase in the average maximum coherence is observed (see Fig. 5a), on which periodic fluctuations with a period of about 1000 days are superimposed (see Fig. 6). This effect was previously discovered in Lyubushin (2020a, 2020c) for using averaged absolute correlations.

It is interesting to note that a period of 1000 days can also be found in the behavior of global seismicity after 2004. Figure 14a shows a graph of the time series of numbers of strong earthquakes with a magnitude of at least 7 in successive time intervals of 50 days from the beginning of 1997 to the end of 2020. Figure 14b shows the time–frequency diagram of the logarithms of the squares of the Morlet wavelet coefficients, in which the occurrence of a periodicity with a period of 1000 days is noticeable since 2004. Thus, the periodic fluctuations of the average measure of coherence in Fig. 5a and the modulation of the numbers of the strongest earthquakes in Fig. 14 with the same periods of about 2.7 years may have a common cause.

In the paper Lyubushin (2020a) it was shown that the maximum coherence between LOD time series and the first principal component of four daily properties of seismic noise (multifractal singularity spectrum support width, generalized Hurst exponent, wavelet based entropy and DJ index within 50 reference points) estimated within moving time window of the length 365 days gains maximum values for time interval 2003–2004. This phenomenon was preceded by strong spike in the value of wavelet-packet measure of non-stationarity of high-frequency LOD component which corresponds to the middle of 2002. These facts provide foundation for hypothesis of trigger influence of anomalies of the Earth's rotation on the break points of the curve at the Fig. 5a and on the occurring of 1000-days periodicity of strongest earthquakes at the Fig. 14. The same effect of high-frequency LOD anomaly was presented in Lyubushin (2020c).

The second critical time interval in the behavior of global seismic noise refers to 2011–2012. After it, chaotic pulsations begin with a high amplitude of the maximum distances between the reference points, for which a strong pairwise coherence arose exceeding the threshold of 0.9 (Fig. 5b), as well as the number of such pairs of control points (Fig. 5d). A similar effect for the entropy of global seismic noise in calculating strong correlations between the values at the control points exceeding the threshold of 0.7 in absolute value was found in Lyubushin (2020c). However, for the average maximum DJ index coherences, this effect is much more pronounced. The existence of the second critical time interval 2011–2012 is also highlighted on the graphs and maps in Figs. 8, 11, 13. It is now impossible to indicate an unambiguous reason for the rearrangement of the spatial structure of seismic noise in the period 2011–2012. In Lyubushin (2020c), the presence of two close mega-earthquakes is indicated as a possible cause of this phenomenon: February 27, 2010, M = 8.8 in Chile and March 11, 2011, M = 9.1 in Japan.

Analyzing the spatial features of the distribution of the DJ index values (Fig. 3), the average maximum coherences (Fig. 8) and the spatial distribution of the responses of the noise properties to the irregularity of the Earth's rotation (the maximum values of the coherence with the LOD time series, Fig. 13), it should be noted that the Arctic region is distinguished either by maximum or minimum values of the analyzed statistics. At the same time, the Arctic stands out most clearly after 2012.

The data analysis technique in this article has a lot of similar features with previously published results of analysis of wavelet-based entropy in Lyubushin (2020c). But the results for DJ-index are much more explicit, especially those which are presented by graphs at Fig. 3b, d. One could notice the "explosion-like" increase of strong maximum coherence values after 2012. In Lyubushin (2020c) this effect could be noticed as well, but it is much weaker. Other strong difference is using frequency-dependent coherence functions instead of usual correlation coefficients which provide a tool to attain much stronger maximum coherence values than maximum absolute correlations (0.9 instead of 0.7). The using of frequency dependent coherences provides extracting "burst-like" effect of increasing strong coherence after 2012.

Regarding the possible geological interpretation of the anomalous zone in the North-East of Siberia, highlighted in Fig. 3a, it can be noted that it partially coincides with the known in geology of the Putorana plateau. This plateau is a completely uninhabited mountain area east of the city of Norilsk, equal in area to Great Britain, and consisting of a network of extinct ancient volcanoes that once poured out lava flows and created the Siberian trap province. Thus, the measure of the non-stationarity of low frequency

seismic noise used in this article unexpectedly highlighted the signs of hidden inner life of a once very active geological structure.

7. Conclusion

A new method for analyzing the properties of low-frequency seismic noise is proposed, based on the calculation of pairwise coherence spectra between the medians of daily noise properties in a network of reference points from a given number of the nearest operational stations. The Donoho-Johnstone index, defined as the fraction of the maximum modulus values of the wavelet coefficients, separating the "noise" coefficients, was chosen as the studied property of noise. The orthogonal wavelet basis is determined from the condition of the minimum entropy of the distribution of the squares of the wavelet coefficients. For observations of seismic noise on the global network of broadband stations in the time interval 1997–2020, two critical time intervals for restructuring the spatial properties of noise have been allocated. The first time interval, 2002.5–2003.5, is characterized by the beginning of an increase in the average noise coherence, the second time interval, 2011–2012, is notable for the appearance of long-range strong coherences exceeding the threshold of 0.9. A new concept of the spatially distributed response of the properties of seismic noise to the irregularity of the Earth's rotation is introduced as the value of the maximum coherence between the time series of the length of the day and the properties of noise in the network of control points, estimated in a sliding time window. By extrapolating noise statistics from a network of reference points to the entire earth's surface, maps of their spatial distribution were obtained. It is shown that bursts of maximum coherence, averaged over a network of reference points, foreshadow seismic energy surges with a medium lead of 530 days.

Acknowledgements

The work was carried out within the framework of the state assignment of the Institute of Physics of the Earth of the Russian Academy of Sciences (topic AAAA-A19-119082190042-5)

References

Ardhuin, F., Stutzmann, E., Schimmel, M., & Mangeney, A. (2011). Ocean wave sources of seismic noise. *Journal of Geophysical Research, 116*, C09004.

Aster, R., McNamara, D., & Bromirski, P. (2008). Multidecadal climate induced variability in microseisms. *Seismological Research Letters, 79*, 194–202.

Bendick, R., & Bilham, R. (2017). Do weak global stresses synchronize earthquakes? *Geophysical Research Letters, 44*, 8320–8327. https://doi.org/10.1002/2017GL074934

Costa, M., Goldberger, A. L., & Peng, C.-K. (2005). Multiscale entropy analysis of biological signals. *Physical Review E, 71*, 021906.

Costa, M., Peng, C.-K., Goldberger, A. L., & Hausdorf, J. M. (2003). Multiscale entropy analysis of human gait dynamics. *Physica A: Statistical Mechanics and Its Applications, 330*, 53–60.

Donoho, D.L., & Johnstone, I. M. (1995). Adapting to unknown smoothness via wavelet shrinkage. *Journal of the American Statistical Association*, *90*(432), 1200–1224. http://statweb.stanford.edu/∼imj/WEBLIST/1995/ausws.pdf

Duda, R. O., Hart, P. E., & Stork, D. G. (2000). *Pattern Classification*. Wiley-Interscience Publication.

Huber, P.J., & Ronchetti, E.M. (2009). *Robust Statistics, 2nd edn*. Wiley. https://doi.org/10.1002/9780470434697.ch1

Kedar, S., Longuet-Higgins, M., Webb, F., Graham, N., Clayton, R., & Jones, C. (2008). The origin of deep ocean microseisms in the North Atlantic Ocean. *Proceedings of the Royal Society A, 464*, 777–793.

Kobayashi, N., & Nishida, K. (1998). Continuous excitation of planetary free oscillations by atmospheric disturbances. *Nature, 395*, 357–360.

Koutalonis, I., & Vallianatos, F. (2017). Evidence of non-extensivity in earth's ambient noise. *Pure and Applied Geophysics., 174*, 4369–4378. https://doi.org/10.1007/s00024-017-1669-9

Levin, B. W., Sasorova, E. V., Steblov, G. M., Domanski, A. V., Prytkov, A. S., & Tsyba, E. N. (2017). Variations of the Earth's rotation rate and cyclic processes in geodynamics. *Geodesy and Geodynamics, 8*(3), 206–212. https://doi.org/10.1016/j.geog.2017.03.007

Lyubushin A. (2018). Synchronization of geophysical fields fluctuations. In: *Complexity of Seismic Time Series: Measurement and Applications*, Editors: Tamaz Chelidze, Luciano Telesca, Filippos Vallianatos, Elsevier 2018, Amsterdam, Oxford, Cambridge. Chapter 6, pp 161–197. https://doi.org/10.1016/B978-0-12-813138-1.00006-7

Lyubushin, A. A. (2014). Analysis of coherence in global seismic noise for 1997–2012. *Izvestiya, Physics of the Solid Earth, 50*(3), 325–333. https://doi.org/10.1134/S1069351314030069

Lyubushin, A. A. (2015). Wavelet-based coherence measures of global seismic noise properties. *Journal of Seismology, 19*(2), 329–340. https://doi.org/10.1007/s10950-014-9468-6

Lyubushin, A. A. (2017). Long-range coherence between seismic noise properties in Japan and California before and after Tohoku mega-earthquake. *Acta Geodaetica Et Geophysica, 52*, 467–478. https://doi.org/10.1007/s40328-016-0181-5

Lyubushin, A. (2020a). Trends of global seismic noise properties in connection to irregularity of earth's rotation. *Pure and Applied Geophysics., 177*, 621–636. https://doi.org/10.1007/s00024-019-02331-z

Lyubushin, A. (2020b). Connection of seismic noise properties in japan and california with irregularity of earth's rotation. *Pure and Applied Geophysics., 177*, 4677–4689. https://doi.org/10.1007/s00024-020-02526-9

Lyubushin, A. (2020c). Global seismic noise entropy. *Frontiers in Earth Science, 8*, 611663. https://doi.org/10.3389/feart.2020.611663

Lyubushin, A. A. (2021a). Seismic noise wavelet-based entropy in Southern California. *Journal of Seismology, 25*, 25–39. https://doi.org/10.1007/s10950-020-09950-3

Lyubushin, A. (2021b). Low-frequency seismic noise properties in the Japanese Islands. *Entropy, 23*, 474. https://doi.org/10.3390/e23040474

Lyubushin, A. A., Kopylova, G. N., & Serafimova, Yu. K. (2021). The relationship between multifractal and entropy properties of seismic noise in Kamchatka and irregularity of the earth's rotation. *Izvestiya, Physics of the Solid Earth, 57*(2), 279–288. https://doi.org/10.1134/S106935132102004X

Mallat, S. (1999). *A Wavelet Tour of Signal Processing* (2nd ed.). Academic Press.

Marple (Jr), S. L. (1987). *Digital Spectral Analysis with Applications*. Prentice-Hall Inc.

Nishida, K., Kawakatsu, H., Fukao, Y., & Obara, K. (2008). Background love and Rayleigh waves simultaneously generated at the Pacific Ocean floors. *Geophysical Research Letters, 35*, L16307.

Nishida, K., Montagner, J., & Kawakatsu, H. (2009). Global surface wave tomography using seismic hum. *Science, 326*(5949), 112.

Rhie, J., & Romanowicz, B. (2004). Excitation of Earth's continuous free oscillations by atmosphere-ocean-seafloor coupling. *Nature, 431*, 552–554.

Shanker, D., Kapur, N., & Singh, V. (2001). On the spatio temporal distribution of global seismicity and rotation of the Earth—A review. *Acta Geodaetica Et Geophysica Hungarica., 36*, 175–187. https://doi.org/10.1556/AGeod.36.2001.2.5

Tanimoto, T. (2001). Continuous free oscillations: Atmosphere-solid earth coupling. *Annual Review of Earth and Planetary Sciences, 29*, 563–584.

Tanimoto, T. (2005). The oceanic excitation hypothesis for the continuous oscillations of the Earth. *Geophysical Journal International, 160*, 276–288.

Vallianatos, F., Koutalonis, I., & Chatzopoulos, G. (2019). Evidence of Tsallis entropy signature on medicane induced ambient seismic signals. *Physica A: Statistical Mechanics and Its Applications, 520*, 35–43. https://doi.org/10.1016/j.physa.2018.12.045

Varotsos, P.A., Sarlis, N.V., & Skordas, E.S. (2011). Natural time analysis: the new view of time. In: *Precursory Seismic Electric Signals, Earthquakes and other Complex Time Series*. Springer-Verlag Berlin Heidelberghttps://doi.org/10.1007/978-3-642-16449-1

Varotsos, P. A., Sarlis, N. V., & Skordas, E. S. (2003a). Long-range correlations in the electric signals that precede rupture: Further investigations. *Physical Review E., 67*, 021109. https://doi.org/10.1103/PhysRevE.67.021109

Varotsos, P. A., Sarlis, N. V., & Skordas, E. S. (2003b). Attempt to distinguish electric signals of a dichotomous nature. *Physical Review E., 68*, 031106. https://doi.org/10.1103/PhysRevE.68.031106

Varotsos, P. A., Sarlis, N. V., Skordas, E. S., & Lazaridou, M. S. (2004). Entropy in the natural time domain. *Physical Review E, 70*, 011106. https://doi.org/10.1103/PhysRevE.70.011106

Xu, C., & Sun, W. (2012). Co-seismic Earth's rotation change caused by the 2012 Sumatra earthquake. *Geodesy and Geodynamics, 3*(4), 28–31. https://doi.org/10.3724/SP.J.1246.2012.00028

Zotov, L., Sidorenkov, N. S., Bizouard, C., Shum, C. K., & Shen, W. (2017). Multichannel singular spectrum analysis of the axial atmospheric angular momentum. *Geodesy and Geodynamics, 8*(6), 433–442. https://doi.org/10.1016/j.geog.2017.02.010

(Received May 17, 2021, revised August 10, 2021, accepted August 17, 2021)